ADVANCED
ENERGY
MATERIALS
www.advenergymat.de

Materials
Views
www.MaterialsViews.com

COMMUNICATION

Open-Cage Fullerenes as n-Type Materials in Organic Photovoltaics: Relevance of Frontier Energy Levels, Carrier Mobility and Morphology of Different Sizable Open-Cage Fullerenes with Power Conversion Efficiency in Devices

Chih-Ping Chen,* Yu-Wei Lin, Jia-Cherng Horng, and Shih-Ching Chuang*

1. Introduction

Harvesting light with greener and renewable approach is the current focus of material researches in the development of solar technology around the globe. The ubiquitous advantages–light weight, flexibility, and economical, low-temperature, and large-area fabrication–displayed by thin-film materials make themselves promising targets for applications in future life.[1–4] Thin-film organic photovoltaics (OPVs), embedding poly(3-hexylthiophene-2,5-diyl) (P3HT) and fullerene derivative,[5–8] [6,6]-phenyl-C_{61} butyric acid methyl ester ($PC_{61}BM$) in the active layer,[9] have been recognized for generating power efficiently under illumination.[10–21] Power conversion efficiency (PCE) of OPVs has been shaped over 6% using the blends of new conjugated polymers and **PCBM**.[22–24] Challenges toward higher PCE to the limits of theoretical values are focused on the use of **PCBM** and its analogues as n-type materials,[25,26] however, only few have been made to develop new fullerene derviatives for OPV applications.[27–34] Li *et al.* recently show that OPVs integrated with indene-C_{60} bisadducts and P3HT exhibit high PCE up to 6.5% through increasing LUMO energy levels of electron acceptors.[35–41]

We envisaged that studies of OPVs have been relied on **PCBM**-type materials for long terms; thus, developing new n-type materials for achieving higher PCE solar cells remains a relatively unexplored topic. We speculate that OPVs integrated with methanofullerenes-type acceptors as **PCBM** may degrade through ring opening process (retro-Bingel reaction),[42] upon long-term exposure to light.[43] Further, developments of new n and p-type materials remain unparallel since many

newly prepared polymers have been using **PCBM** as standard n-type partners for evaluation of their photovoltaic efficiency. Advanced improvement of efficiency has seen lacking choices of frontier orbital energy level-matched n-type materials. In addition, an efficient integrated active layer requires n,p-materials with balanced carrier mobility for reduction of the space charge which causes carriers recombination, and with suitable solubility for morphology control.[31,44,45] Thus, we have directed our goal toward a series of non-methanofullerenes-type materials that exhibit distinguishable optoelectronic properties.[46] The explored derivatives feature non-methanofullerenes that are relatively more stable for OPV applications. In this paper, we report a new series of open-cage fullerenes possessing suitable solubilizing functionality with a variety of frontier molecular orbital energy levels and carrier mobility as n-type materials, and evaluate their performances upon embedded in the active layers with P3HT in the device. The mystery of photovoltaic application using open-cage fullerenes is disclosed in this study.

First, we efficiently prepared open-cage fullerenes **4** starting with [4 + 2] cycloaddition of diazene **3** with C_{60} in 1-chloronaphthalene at 270 °C (**Figure 1**). The diazene **3** was synthesized by an inverse-electron demand Diels-Alder reaction of bis(2-thienyl)tetrazine (**1**) with hept-6-enoic acid ethyl ester (**2**) followed by oxidation. Open-cage fullerenes **5a,b**, derivatized from **4** by O_2 oxidation featuring a 12-membered-ring opening, consisted of isomeric structures of **5a/5b** in 60/40 molar ratio by ^1H NMR analyses. Derivatives **6a,b**, **7a,b** and **8a,b**,[47] with 13, 16 and 20-membered-ring orifices respectively, were prepared through reaction of a mixture of **5a,b** with sulfur/TDAE, hydrazine/pyridine and o-phenylenediamine/pyridine by carbon-carbon bond scissions respectively; their isomeric molar ratios, in 60/40, 57/43 and 51/49 respectively, were determined by ^1H NMR spectroscopy.[48] These open-cage fullerenes were characterized using infrared (IR) and ^1H nuclear magnetic resonance (NMR) spectroscopy, and MALDI-TOF mass spectrometry.[49–53] The isolated compounds are soluble in CS_2, $CHCl_3$, and o-dichlorobenzene (o-DCB); compounds **7a,b** are relatively lower in solubility than compounds **4**, **5a,b**, **6a,b**, and **8a,b** in these solvents.

The electronic properties of these open-cage fullerenes **4**, **5a,b**, **6a,b**, **7a,b** and **8a,b** are revealed from their UV–vis spectra and electrochemical studies. Figure S1 (see SI, the Supporting Information) displays UV-vis spectra of the studied open-cage fullerenes and $PC_{61}BM$. We observe that the molar absorptivities in the visible region (450–740 nm)

Dr. C.-P. Chen
Materials and Chemical Laboratories
Industrial Technology Research Institute
195, Sec. 4, Chung Hsing Road, Chutung, Hsinchu, 310, Taiwan, R.O.C.
E-mail: chihping_chen@itri.org.tw
Mr. Y.-W. Lin, Prof. S.-C. Chuang
Department of Applied Chemistry
National Chiao Tung University
Hsinchu, 300, Taiwan, R.O.C.
E-mail: jscchuang@faculty.nctu.edu.tw
Prof. J.-C. Horng
Department of Chemistry
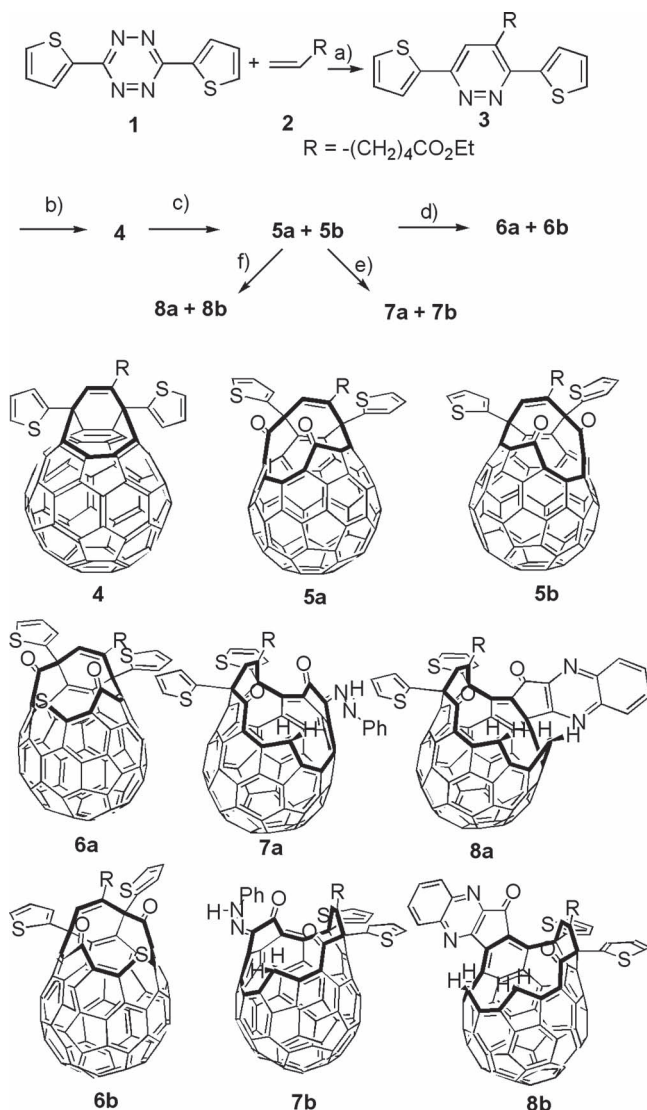National Tsing Hua University
Hsinchu, Taiwan, R.O.C. 300

Figure 1. Synthesis of open-cage fullerenes **4**, **5a,b**, **6a,b**, **7a,b** and **8a,b**. Conditions a) *o*-xylene, 140 °C, 24 h (in pressured tube); then bubbling O_2 for 15 min; *o*-xylene, 140 °C, 24 h again (39%); b) C_{60}, 1-chloronaphthalene, reflux, 48 h (39%; 85% based on converted C_{60}); c) O_2, CS_2, *hν*, 3 h (67%); d) tetrakis(dimethylamino)ethene (TDAE), *o*-DCB, 180 °C, 10 min (91%); e) phenylhydrazine, pyridine, *o*-DCB, 65 °C, 2 h (49%); f) *o*-phenylenediamine, pyridine, *o*-DCB, 65 °C, 18 h (69%).

for compound **7a,b** are exceptionally intense, while those of **4** and **8a,b** are relatively weak; compound **5a,b** and **6a,b** exhibit featureless absorptions beyond 450 nm. The unusual absorption displayed by **7a,b** is more intense than that exhibited by [6,6]-phenyl-C_{71} butyric acid methyl ester (**PC$_{71}$BM**) in the visible region, and it may be efficient in enhancing short circuit currents in the device through improved light absorption.[54] The intense absorptions in the visible region exhibited by compound **7a,b** and **8a,b** are likely due to their higher extent of disruption from spherical π-surface, leading to higher degree of planar π-conjugation. It is also noteworthy that the absorption patterns of **4** resemble those of **PC$_{61}$BM** although they possess structurally different

features–bisfulleroids (**4**) versus homoconjugated fullerenes (**PC$_{61}$BM**).

Next, we used cyclic voltammetry (CV, Figure S2, see SI) to examine the redox properties of **4**, **5a,b**, **6a,b**, **7a,b** and **8a,b**. Table S1 lists the half-wave reduction potentials relative to ferrocene/ferrocenium, LUMO energy level, band gap, HOMO energy level of these studied compounds. We found that compound **5a,b**, with its lower LUMO energy level at −4.01 eV, are exceptionally easier to be reduced than all the other open-cage compounds, likely due to the joint enone moieties; the observed LUMO energy levels descend in the order of **7a,b** > **4** > **PC$_{61}$BM** > **6a,b** > **8a,b** > **5a,b**. Due to the lower LUMO energy level, compound **5a,b** are rather reactive toward nucleophiles; consequently, compound **6a,b**, **7a,b** and **8a,b**, derivatized from **5a,b**, possess higher LUMO energy levels for lack of combined enone moieties. **Figure 2**a shows the energy level diagram determined from the onset potential of the first reductions and onset absorption from UV-vis spectra for all compounds. The bandgaps of **5a,b**, **7a,b** and **8a,b** are relatively smaller than those of **PC$_{61}$BM**, **4** and **6a,b**. According to these results, we would expect that **7a,b** exhibit the largest open-circuit voltage (V_{oc}) with P3HT in the device among the studied compounds. The V_{oc} is determined by the difference of the HOMO energy level of P3HT to the LUMO energy level of open-cage fullerenes; the higher LUMO levels (with more cathodic shifts) of the open-cage fullerene derivatives correspond to higher values of V_{oc} in the fabricated devices.[22–24]

We fabricated photovoltaic cells by spin-coating the blends of open-cage fullerenes and P3HT in *o*-DCB solution with layering configuration of glass/ITO/PEDOT:PSS/P3HT:fullerenes/Ca/ Al using known protocols.[55–57] **Table 1** summarizes the performances of the OPV devices incorporating **PC$_{61}$BM**, **4**, **5a,b**, **6a,b**, **7a,b**, **8a,b** and P3HT (see Figure 2b for *J–V* plots). Their best PCEs are all above 1.1% and not well correlated with their cage sizes; except for the compound **5a,b** with extraordinarily low LUMO energy, the observed PCEs decrease as compound cage-size increases. The observed relative order of V_{oc} values, **7a,b** > **4** > **8a,b** > **6a,b** > **5a,b**, are correlated with their LUMO energy levels, excepting for the relative order of **6a,b** and **8a,b**. To our delight, open-cage fullerene **4** exhibited the best and reproducible performance value of 2.9% among the open-cage compounds with P3HT (*ca*. 10% less than that of a standard cell with **PC$_{61}$BM**/P3HT recorded at the same condition; Table 1, entries 1–2), with typical V_{oc} of 0.62 ± 0.02 V, J_{sc} of 7.1 ± 0.1 mAcm^{-2}, and FF of 64 ± 2%. As expected, compound **5a,b** displayed lower best PCE at 1.3% with lowest V_{oc} of 0.40 ± 0.01 V among all compounds due to its low LUMO energy level (entry 3). Upon raising 0.20 eV of the LUMO energy level through insertion of a sulfur atom in the rim of **5a,b** to give **6a,b**, best PCE was improved about 0.5% with an increment of V_{oc} of 0.11 V (entry 4). We found that the performances of these open-cage fullerenes were also not consistent with their relative order of LUMO energy levels. Despite of its higher LUMO energy levels, the device performance shown by **7a,b**/P3HT is dissatisfying since compound **7a,b** tends to form precipitates in *o*-DCB solution during film formation, likely due to intermolecular hydrogen bonding through N-H. Its best performance of 1.7% was recorded with a concentration of 10 mgmL^{-1} of **7a,b** for establishing a reasonable device (entry 5). It is noteworthy
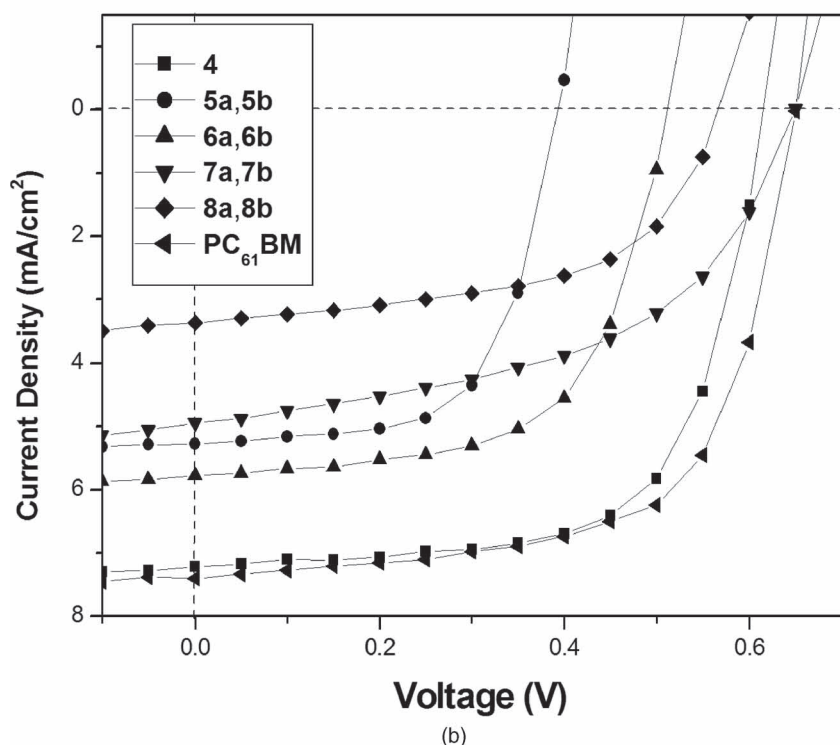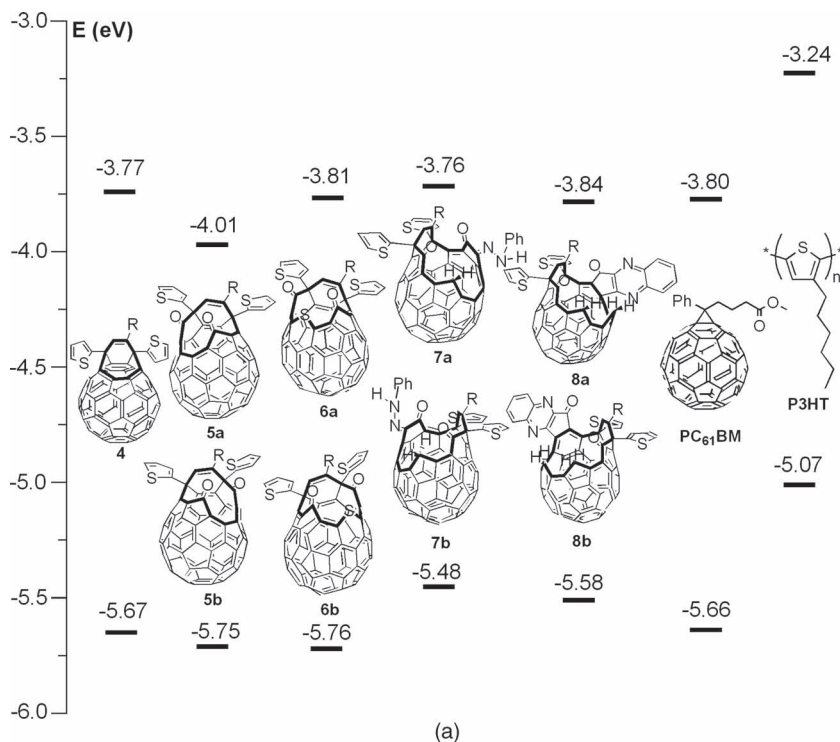
ADVANCED
ENERGY
MATERIALS
www.advenergymat.de

Materials
Views
www.MaterialsViews.com

COMMUNICATION

(a)

(b)

Figure 2. (a) Energy level diagram of $PC_{61}BM$, **4**, **5a,b**, **6a,b**, **7a,b**, **8a,b** and P3HT. (b) $J–V$ curves of **4**, **5a,b**, **6a,b**, **7a,b**, **8a,b** and P3HT best OPV devices.

The irregularity of PCEs of these open-cage fullerenes with P3HT showed that their LUMO energy levels (or V_{oc}) may not be the only factor determining their device performances. Other parameters are relevant in revealing their relative orders. In general, an efficient device requires balanced and higher hole or electron mobility in active layer for effective carrier transport.[48] An electron-only device structure, configured of ITO/Al/P3HT:fullerenes/Ca/Al, is adopted to extract the electron mobility of respective films for comparison. When a sufficient voltage is applied to the electron-only devices, the transport of electron through the blend film is limited by the space charge that accumulates. The space charge limited current (SCLC) is described by equation 1, where ε_r, ε_0, μ_e, V and L denote electric constant of the materials, the permittivity of free space, the electron mobility, the voltage applied to the device, and the blend film thickness, respectively.

$$J = \frac{9}{8}\varepsilon_r\varepsilon_0\mu_e\frac{V^2}{L^3} \tag{1}$$

Figure S3 (SI) displays the experimental dark-current densities measured in the electron-only devices. The applied voltage (V_{appl}), estimated from the difference in electrical contact work functions, is corrected for the built-in voltage ($V_{bi} = 1.4$ V). The plots of $J^{0.5}$ versus V for each device were nearly a straight line, providing a slope that we used it to calculate the field-independent mobility of open-cage fullerenes (Table 1 and Table S2). We found that electron mobility of the fabricated films decreased as the active layer was blended with larger-orifice open-cage fullerenes; in this study, compound **4** exhibited mobility of $5.2 \pm 0.1 \times 10^{-8}$ m^{2}V^{-1}s^{-1}, close to that of $PC_{61}BM$, and the 20-membered-ring compound **8a,b** displayed an order less mobility, $7.1 \pm 0.1 \times 10^{-9}$ m^{2}V^{-1}s^{-1}. The low electron mobility incorporating **8a,b** may be attributed to its relatively more ruptured π-structure or more likely the presence of spontaneously encapsulated water in **8a,b** that decreases the carrier transportation. Our results show that current density (J_{sc}) of an OPV device was in parallel to SCLC electron mobility and thus are well correlated with their cage sizes. As a result, the electron mobility can be manipulated through rupturing the extent of π–π conjugation of the fullerene π-surface. From another aspect in terms of balanced carriers transport for efficient photovoltaics,[44,45] this series of open-cage fullerene materials may provide choices of n-type materials with more flexibility and compatibility for new p-type materials.

that the largest cage compound **8a,b** showed the worst performance with P3HT (entry 6), which is likely due to the higher extent of the ruptured π-structure that reduces the charge transport potential.[38]

Table 1. J–V characteristics of devices incorporating $PC_{61}BM$, **4**, **5a,b**, **6a,b**, **7a,b** and **8a,b** and P3HT (1:1, w/w).[a]

entry	compound	J_{sc}[b]	V_{oc} (V)	FF	Ave PCE (%)	Best PCE (%)	μ_e[c]
1	$PC_{61}BM$	7.4 ± 0.3	0.64 ± 0.01	0.66 ± 0.01	3.1	3.2	8.6 ± 0.2 × 10^{-8}
2	**4**	7.1 ± 0.1	0.62 ± 0.02	0.64 ± 0.02	2.8	2.9	5.2 ± 0.1 × 10^{-8}
3	**5a,b**	4.9 ± 0.3	0.40 ± 0.01	0.63 ± 0.01	1.2	1.3	3.9 ± 0.3 × 10^{-8}
4	**6a,b**	5.7 ± 0.1	0.51 ± 0.01	0.61 ± 0.01	1.7	1.8	2.8 ± 0.6 × 10^{-8}
5	**7a,b**[d]	4.9 ± 0.1	0.65 ± 0.01	0.51 ± 0.01	1.6	1.7	1.6 ± 0.3 × 10^{-8}
6	**8a,b**[e]	3.5 ± 0.1	0.57 ± 0.01	0.56 ± 0.01	1.1	1.2	7.1 ± 0.1 × 10^{-9}

[a]Data collected with concentration at 15 mgmL^{-1} in o-DCB and film spin coated at 800 rpm unless otherwise noted; data obtained from 10 individual devices for each entry; [b]Current density (mAcm^{-2}); [c]Units in m^{2}V^{-1}s^{-1}; values are determined from SCLC method; [d]Concentration of **7a,b** in 10 mgmL^{-1}. e) Film spin coated at 1200 rpm.

We further scrutinized the topographies and phase diagrams of blend films incorporating each open-cage fullerene with P3HT by atomic force microscopy (AFM) in the tapping mode. AFM phase images of two-component blend film further provide clues regarding the surface hardness. The hard domains, attributing to polymer domains, appear as bright regions, whereas the dark regions denote the soft segments that correspond to fullerene domains.[57,58] As shown in **Figure S4** in SI, all blend films display relatively low levels of root mean square (RMS) roughness (<5 nm) with nearly no aggregations. The relatively higher PCE of the device incorporating **4**/P3HT appears to correlate with its well-separated P3HT and **4** domains (RMS = 3.8 nm) featuring self-organized fibrillar P3HT (Figure S5, SI).

To conclude, we have efficiently synthesized open-cage fullerenes possessing different orifice-size ranging from eight to twenty-membered-ring and demonstrated their OPV performances incorporating these new n-type materials. We found that their PCEs are dependent on the frontier energy level and highly associated with their electron mobilities in devices. The device with PCE up to 2.9%, shown by the eight-membered-ring compound/P3HT with high fill factor of 66%, was obtained. The eight-membered-ring fullerene with suitable solubilizing groups features a bisfulleroid moiety—bis-[5,6]-open moiety—on fullerene cage, providing previously unavailable candidates for OPVs application. This work also first uncovers the mystery between the extents of the ruptured π-structures of fullerenes with their resulting electronic properties. To the best of our knowledge, this is the first demonstration of high performance OPVs incorporating open-cage fullerenes as n-type materials. Currently, we are fine-tuning the blend morphology by tailoring the functionality of open-cage fullerenes and evaluating the compatibility with other conjugated polymers toward higher PCE.

2. Experimental Section

2.1. Materials and Equipment for Polymer Solar Cells

General methods: All reactions were performed under argon. Dry o-DCB was distilled from CaH$_2$ under argon. The chemical shifts of ^{1}H and ^{13}C NMR are with reference to tetramethylsilane (TMS) or CHCl$_3$. All chemicals were purchased and used as received unless otherwise noted.

Photovoltaic Cells Fabrication and Testing: All BHJ (bulk heterojunction) photovoltaic devices were prepared with same procedures. The device

fabrication procedures are described below: the glass-indium tin oxide (ITO) substrates (obtained from Sanyo, Japan (8Ω/□)) were first patterned by lithography, then cleaned with detergents, ultrasonicated in acetone and isopropyl alcohol and subsequently dried on hot plate at 120 °C for 5 min, and finally treated with oxygen plasma for 5 min. Poly(3,4-ethylene-dioxy-thiophene):poly(styrenesulfonate) (PEDOT:PSS, Baytron P-VP AI4083) was filtered through a 0.45 μm filter before being deposited on ITO, with a thickness around 30 nm, by spin coating at 3000 rpm in the air and dried at 150 °C for 30 min inside glove box. The devices were fabricated using the synthesized open-cage fullerenes at a concentration of 15 mgmL^{-1} (weight ratio of open-cage fullerenes to P3HT: 1:1), a spin rate of 800 rpm for 30 s, and o-DCB as the solvent. The optimal thickness of the active layers obtained under these conditions was *ca.* 150 nm. Subsequently, the device was completed by coating 30 nm-thick of Ca and an 80 nm-thick of Al in < 10^{-6} mm-Hg pressure, respectively. The active area of the device is 5 mm^2. Finally the cell was encapsulated using UV-curing glue (obtained from Nagase, Japan). During the encapsulation process, the UV-glue was dispensed onto the edge of a piece of glass in the air. The UV-glue coated glass was transferred to the glove box for covering the OPV device. The device was then sealed by pressing the UV-glue coated glass on top of the device, and the device underwent UV curing (254 nm) for 2 min. Upon device encapsulation, the I–V curves of the OPV devices were measured in air, using a computer-controlled Keithley 2400 source measurement unit (SMU) equipped with a Peccell solar simulator under AM 1.5G illumination (100 mWcm^{-2}). The illumination intensity was calibrated using a standard Si photodiode detector equipped with a KG-5 filter. The output photocurrent was adjusted to match the photocurrent of the Si reference cell to obtain a power density of 100 mWcm^{-2}. After encapsulation, all devices measurements were operated in an ambient atmosphere at 25 °C. The efficiency of a P3HT/PCBM reference cell, 3.5% measured under illumination in our laboratory, was verified to be 3.4% under AM1.5G conditions (100 mWcm^{-2}) in National Institute of Advanced Industrial Science and Technology (AIST, Japan). The morphologies of the polymer films were analyzed using a VEECO DICP-II atomic force microscope operated in the dynamic force mode at ambient temperature and an etched Si probe operated under a resonant frequency of 131 kHz and a spring constant of 11 Nm^{-1}. The device fabrication procedure is the same for construction of the electron only devices.

Supporting Information

Supporting Information is available from the Wiley Online Library or from the author.

Acknowledgements

ADVANCED
ENERGY
MATERIALS

www.advenergymat.de

Materials
Views

www.MaterialsViews.com

COMMUNICATION

[1] M. Helgesen, R. Søndergaard, F. C. Krebs, *J. Mater. Chem.* **2010**, *20*, 36.

[2] F. C. Krebs, S. A. Gevorgyan, J. Alstrup, *J. Mater. Chem.* **2009**, *19*, 5442.

[3] F. C. Krebs, *Sol. Energy Mater. Sol. Cells* **2009**, *93*, 465.

[4] L. Blankenburg, K. Schultheis, H. Schache, S. Sensfuss, M. Schrödner, *Sol. Energy Mater. Sol. Cells* **2009**, *93*, 476.

[5] F. Diederich, M. Gomez-Lopez, *Chimia* **1998**, *52*, 551.

[6] F. Diederich, M. Gomez-Lopez, *Chem. Soc. Rev.* **1999**, *28*, 263.

[7] A. Hirsch, M. Brettreich, *Fullerenes: Chemistry and Reactions*, Wiley-VCH, Weinheim, **2005**.

[8] C. Thilgen, F. Diederich, *Chem. Rev.* **2006**, *106*, 5049.

[9] J. C. Hummelen, B. W. Knight, F. LePeq, F. Wudl, *J. Org. Chem.* **1995**, *60*, 532.

[10] N. S. Sariciftci, L. Smilowitz, A. J. Heeger, F. Wudl, *Science* **1992**, *258*, 1474.

[11] G. Yu, J. Gao, J. C. Hummelen, F. Wudl, A. J. Heeger, *Science* **1995**, *270*, 1789.

[12] S. E. Shaheen, C. J. Brabec, N. J. Sariciftci, F. Padinger, T. Fromherz, J. C. Hummelen, *Appl. Phys. Lett.* **2001**, *78*, 841.

[13] C. J. Brabec, N. S. Sariciftci, J. C. Hummelen, *Adv. Funct. Mater.* **2001**, *11*, 15.

[14] N. Camaioni, G. Ridolfi, G. Casalbore-Miceli, A. Possamai, M. Maggini, *Adv. Mater.* **2002**, *14*, 1735.

[15] P. Schillinsky, C. Waldauf, C. J. Brabec, *Appl. Phys. Lett.* **2002**, *81*, 3885.

[16] M. M. Wienk, J. M. Kroon, W. J. H. Verhees, J. Knol, J. C. Hummelen, P. A. van Hal, R. A. J. Janssen, *Angew. Chem. Int. Ed.* **2003**, *42*, 3371.

[17] F. Padinger, R. Rittberger, N. S. Sariciftci, *Adv. Funct. Mater.* **2003**, *13*, 85.

[18] F. L. Zhang, M. Johansson, M. L. Andersson, J. C. Hummelen, O. Inganas, *Synth. Met.* **2003**, *137*.

[19] J.-F. Nierengarten, *New J. Chem.* **2004**, *28*, 1171.

[20] G. Li, V. Shrotriya, J. Huang, Y. Yao, T. Moriarty, K. Emery, Y. Yang, *Nat. Mater.* **2005**, *4*, 864.

[21] J. Y. Kim, K. Lee, N. E. Coates, D. Moses, T.-Q. Nguyen, M. Dante, A. J. Heeger, *Science* **2007**, *317*, 222.

[22] Y.-C. Chen, C.-Y. Yu, Y.-L. Fan, L.-I. Hung, C.-P. Chen, C. Ting, *Chem. Commun.* **2010**, *46*, 6503.

[23] S. H. Park, A. Roy1, S. Beaupré, S. Cho, N. Coates, J. S. Moon, D. Moses, M. Leclerc, K. Lee, A. J. Heeger, *Nature photon.* **2009**, *3*, 297.

[24] H. Y. Chen, J. Hou, S. Zhang, Y. Liang, G. Yang, Y. Yang, L. Yu, Y. Wu, G. Li, *Nature Photon.* **2009**, *3*, 649.

[25] M. C. Scharber, D. Mühlbacher, M. Koppe, P. Denk, C. Waldauf, A. J. Heeger, C. J. Brabec, *Adv. Mater.* **2006**, *18*, 789.

[26] L. M. Popescu, P. van't Hof, A. B. Sieval, H. T. Jonkman, J. C. Hummelen, *Appl. Phys. Lett.* **2006**, *89*, 213507.

[27] L. P. Zheng, Q. M. Zhou, X. Y. Deng, M. Yuang, G. Yu, Y. Cao, *J. Phys. Chem. B.* **2004**, *108*, 11921.

[28] S. A. Backer, K. Sivula, D. F. Kavulak, J. M. J. Fréchet, *Chem. Mater.* **2007**, *19*, 2927.

[29] F. B. Kooistra, J. Knol, F. Kastenberg, L. M. Popescu, W. J. H. Verhees, J. M. Kroon, J. C. Hummelen, *Org. Lett.* **2007**, *9*, 551.

[30] C. Yang, J. Y. Kim, S. Cho, J. K. Lee, A. J. Heeger, F. Wudl, *J. Am. Chem. Soc.* **2008**, *130*, 6444.

[31] P. A. Troshin, H. Hoppe, J. Renz, M. Egginger, J. Y. Mayorova, A. E. Goryachev, A. S. Peregudov, R. N. Lyubovskaya, G. Gobsch, N. S. Sariciftci, V. F. Razumv, *Adv. Funct. Mater.* **2009**, *19*, 779.

[32] F. B. Kooistra, V. D. Mihailetchi, L. M. Popescu, D. Kronholm, P. W. M. Blom, J. C. Hummelen, *Chem. Mater.* **2006**, *18*, 3068.

[33] T. Niinomi, Y. Matsuo, M. Hashiguchi, Y. Sato, E. Nakamura, *J. Mater. Chem.* **2009**, *19*, 5804.

[34] R. D. Kennedy, A. L. Ayzner, D. D. Wanger, C. T. Day, M. Halim, S. I. Khan, S. H. Tolbert, B. J. Schwartz, *J. Am. Chem. Soc.* **2008**, *130*, 17290.

[35] Y. J. He, H.-Y. Chen, J. H. Hou, Y. F. Li, *J. Am. Chem. Soc.* **2010**, *132*, 5532.

[36] G. J. Zhao, Y. J. He, Y. F. Li, *Adv. Mater.* **2010**, *22*, 4355.

[37] M. Lenes, G. J. A. H. Wetzelaer, F. B. Kooist, S. C. Veenstra, J. C. Hummelen, P. W. M. Blom, *Adv. Mater.* **2008**, *20*, 2116.

[38] M. Lenes, S. W. S. Helton, A. B. Sieval, D. F. Kronholm, J. C. Hummelen, P. W. M. Blom, *Adv. Funct. Mater.* **2009**, *19*, 3002.

[39] R. B. Ross, C. M. Cardona, D. M. Guldi, S. G. Sankaranarayanan, M. O. Reese, N. Kopidakis, J. Peet, B. Walker, G. C. Bazan, E. V. Keuren, B. C. Holloway, M. Drees, *Nat. Mater.* **2009**, *8*, 208.

[40] J. A. Mikroyannidis, A. N. Kabanakis, S. S. Sharma, G. D. Sharma, *Adv. Funct. Mater.* **2011**, *21*, 746.

[41] D. W. Laird, R. Stegamat, H. Richter, V. Vejins, L. Scott, T. A. Lada, Patent WO 2008/018931 A2.

[42] R. Kessinger, M. Gómez-López, C. Boudon, C. J.-P. Gisselbrecht, M. Gross, L. Echegoyen, F. Diederich, *J. Am. Chem. Soc.* **1998**, *120*, 8545.

[43] M. O. Reese, A. J. Morfa, M. S. White, N. Kopidakis, S. E. Shaheen, G. Rumbles, D. S. Ginley, *Sol. Energy Mater. Sol. Cells* **2005**, *86*, 499.

[44] C. Melzer, E. J. Koop, V. D. Mihailetchi, P. W. M. Blom, *Adv. Funct. Mater.* **2004**, *12*, 865.

[45] V. D. Mihailetchi, H. X. Xie, B. de Boer, L. A. J. Koster, P. W. M. Blom, *Adv. Funct. Mater.* **2006**, *16*, 699.

[46] C.-P. Chen, C. Luo, C. Ting, S.-C. Chuang, *Chem. Commun.* **2011**, *47*, 1845.

[47] Compound **8a** and **8b** each encapsulates a water molecule inside the cage in 79% and 54% ratio by ^{1}H NMR analyses, in which encapsulated H_2O appear at −11.28 and −11.34 ppm, respectively.

[48] Compound **5a,b**, **6a,b**, **7a,b** and **8a,b** are isolated as isomeric mixtures since they are difficult to be separated by flash column chromatography in low polarity solvents (toluene/hexanes = 1:1). Later, we find that their solubilities are even lower upon separated from their isomeric mixtures with Buckyprep column by HPLC; mixtures of separated isomers/P3HT do not form better films as isomeric mixtures in devices.

[49] Y. Murata, M. Murata, K. Komatsu, *Chem.–Eur. J.* **2003**, *9*, 1600.

[50] S.-I. Iwamatsu, F. Ono, S. Murata, *Chem. Commun.* **2003**, 1269.

[51] S. Iwamatsu, T. Uozaki, K. Kobayashi, S. Re, S. Nagase, S. Murata, *J. Am. Chem. Soc.* **2004**, *126*, 2668.

[52] L. Gan, D. Yang, Q. Zhang, H. Huang, *Adv. Mater.* **2010**, *22*, 1498.

[53] Y. He, Y. Li, *Phys. Chem. Chem. Phys.* **2011**, *13*, 1970.

[54] M. M. Wienk, J. M. Kroon, W. J. H. Verhees, J. Knol, J. C. Hummelen, P. A. van Hal, R. A. J. Janssen, *Angew. Chem. Int. Ed.* **2003**, *42*, 3371.

[55] P3HT:open-cage fullerenes (15 mgmL[−1], 1:1 w/w) except for **7a,b** using 10 mgmL[−1]. C.-P. Chen, S.-H. Chan, T.-C. Chao, C. Ting, B.-T. Ko, *J. Am. Chem. Soc.* **2008**, *130*, 12828.

[56] C.-Y. Yu, C.-P. Chen, S.-H. Chan, G.-W. Hwang, C. Ting, *Chem. Mater.* **2009**, *21*, 3262.

[57] S.-H. Chan, Y.-S. Hsiao, L.-I. Hung, G.-W. Hwang, H.-L. Chen, C. Ting, C.-P. Chen, *Macromolecules* **2010**, *43*, 3399.

[58] A. J. Moul, K. Meerholz, *Adv. Mater.* **2008**, *20*, 240.